Dynamic modeling of an upper limb hybrid exoskeleton for simulations of load-lifting assistance

Gull, Muhammad Ahsan; Bak, Thomas; Bai, Shaoping

Published in:
Proceedings of the Institution of Mechanical Engineers, Part C: Journal of Mechanical Engineering Science

DOI (link to publication from Publisher):
10.1177/09544062211024687

Publication date:
2022

Document Version
Accepted author manuscript, peer reviewed version

Transportation Research Record
2020, Vol. XX(X) 1–12

DOI: 10.1177/ToBeAssigned
journals.sagepub.com/home/trr
SAGE

Dynamic Modeling of an Upper Limb Hybrid Exoskeleton for Simulations of Load-Lifting Assistance

Muhammad Ahsan Gull[1], Thomas Bak[2] and Shaoping Bai[1]

Abstract

Work-related musculoskeletal disorders (MSDs) are among the most commonly reported issue in Europe. By using robotic exoskeletons to support the user in performing heavy industrial tasks can effectively mitigate the work-related MSDs. In this paper, a dynamic model of a hybrid exoskeleton is presented to analyze the assistive effect. The exoskeleton in this study is able to passively support the human shoulder joint and actively support the human forearm movements by providing the different levels of assistive torque. With the model, two different tasks are simulated, i.e., an overhead lifting task and a static load transferring task. The results show that the assistive torque provided by the passive spring-loaded mechanism has reduced the maximum human upper arm effort by 22.65%. Moreover, the exoskeleton elbow joint's assistive torque has reduced the peak human forearm effort from 10.12 N-m to 5.1 N-m.

Keywords

Upperbody Exoskeleton, Industrial Exoskeleton, Hybrid Exoskeleton, Power sharing, Power amplification, Multibody modeling.

Introduction

Robotic technology has significantly reduced human physical efforts in the harsh industrial environment, such as transporting the load on the factory floor, handling heavy equipment, and transferring heavy objects to other locations. However, robots cannot be entirely possible to eradicate human involvement in the industrial tasks. Several industrial tasks require manual handling of the heavy objects, where the human may have to maintain a prolonged body posture. These tasks can induce muscular fatigue and increase the likelihood of developing different types of musculoskeletal disorders (MSDs) (*1*, *2*). MSDs are among the most commonly reported issue in Europe. According to European Agency for Safety and Health at Work (EU-OSHA), almost 60% of the European workers are experiencing some signs of backache and upper limb pain (*3*). Therefore, one of the research focuses is on development of a variety of exoskeletons to support the user in performing different types of industrial tasks such as handling heavy objects on the shop floor, maintaining a prolonged posture, and transporting the load to a shorter distance by preventing the musculoskeletal disorder.

Wearable exoskeletons have been widely investigated for medical rehabilitation and military applications (*4*–*7*). Recent review highlighted the potential of these devices in many industrial applications as well (*8*). Studies have shown the significance of using an exoskeleton robot to reduce the human muscle effort and fatigue level along with an enhancement in human performance (*11*–*13*).On the other hand, exoskeletons also show some undesirable consequences such as increased loading effect and discomfort on the other parts of the human body(*14*), which needs to be minimized at design stage. Different design approaches, including active, passive, and semi-passive mechanisms, have been adopted to develop a variety of exoskeletons robots. The active exoskeletons can generate higher assistive torques and provide a variable torque profile, but their size and weight have made it difficult to be used in industrial applications compared to their passive and semi-passive counterparts (*15*). On the other hand, passive exoskeletons are lighter and do not require motors and external source of power, such as batteries. There are already commercial passive exoskeletons available in the market, MATE Exoskeleton by Comau, ShoulderX V3 (SuitX, Emeryville, CA, USA), Paexo Shoulder developed by Ottobock, Ekso vest developed

[1]Department of Materials and Production, Aalborg University, Aalborg 9220, Denmark.
[2]Department of Electronics Systems, Aalborg University, Aalborg 9220, Denmark.

Corresponding author:
Muhammad Ahsan Gull and Shaoping Bai, Department of Materials and Production, Aalborg University, Aalborg 9220, Denmark.
Email: mag@mp.aau.dk; shb@mp.aau.dk

Figure 1. The prototype for the upper limb exoskeleton.

by Ekso Bionics, EXHAUSS system (EXHAUSS, France), BESK G exoskeleton developed by developed by GOGOA and SkelEx (SkelEX, Rotterdam, Netherlands) are some examples.

Studies on passive exoskeletons have also been conducted to minimize the human muscle effort specifically for the anterior and middle deltoid muscles(*16, 17*). Kim et al. (*16*) investigated the influence of Ekso vest for arm elevation tasks. The performance of Ekso vest was assessed for overhead drilling and light assembling tasks. It was observed that the shoulder peak muscular activity was reduced by 45%. Pacifico et al. (*18*) studied the effectiveness of proto-Mate designed for the partial compensating of the human arm weight. The experimental data exhibited an overall reduction of human muscle activation by 43%. Karim et al. (*17*) investigated the intervention of three different exoskeletal designs and compared them for a simulated overhead task. ShoulderX^{TM} (suitX^{TM}), FORTIS^{TM} (from Lockheed Martin), and an exoskeleton Vest (by Fawcett Exo-Vest) were compared in terms of physical effort and perceived discomfort using surface EMG. Experimental data showed that FORTIS and Fawcett Exo-Vest had elevated the loading effect on the lower back. In comparison, this loading effect appeared to be more prominent when FORTIS was used for counterbalancing and transferring the load to the ground. However, ShoulderX maintained good task quality and reduced the peak loading. Hyun et al. (*11*) presented a novel multi-linkage energy storing mechanism for an upper-limb exoskeleton (H-VEX) that preserves the shoulder misalignment without using a redundant degree of freedom. Further, to study the effectiveness of this exoskeleton, two overhead drilling tasks were designed, and surface EMG was used to analyze the six upper limb muscles. Grazi et al.(*15*) developed a semi-passive shoulder exoskeleton called H-Pulse, where a novel active mechanism improves the capability of a passively actuated shoulder exoskeleton by automatically modulating the assistive torque. The experimental evaluation of H-Pulse has shown its significance for prolonged overhead lifting tasks and reduced physical human effort.

Some existing works address design issues at the shoulder joint (*9–11*), and some potential solutions that can replicate the human shoulder biomechanics were proposed. The elbow joint, while essential for load lifting and carrying, has been overlooked in most commercial solutions. RoboMate is the only industrial solution that has considered the elbow joint for lifting and transporting the load, but it is comparatively bulkier, and one cannot use it in the narrow workspace that usually exists on the shop floor.

An upper limb hybrid exoskeleton by combining a passive actuated shoulder exoskeleton with a low power active elbow joint module was developed at Aalborg University, Denmark, shown in Fig. 1. A hybrid exoskeleton in this work is a

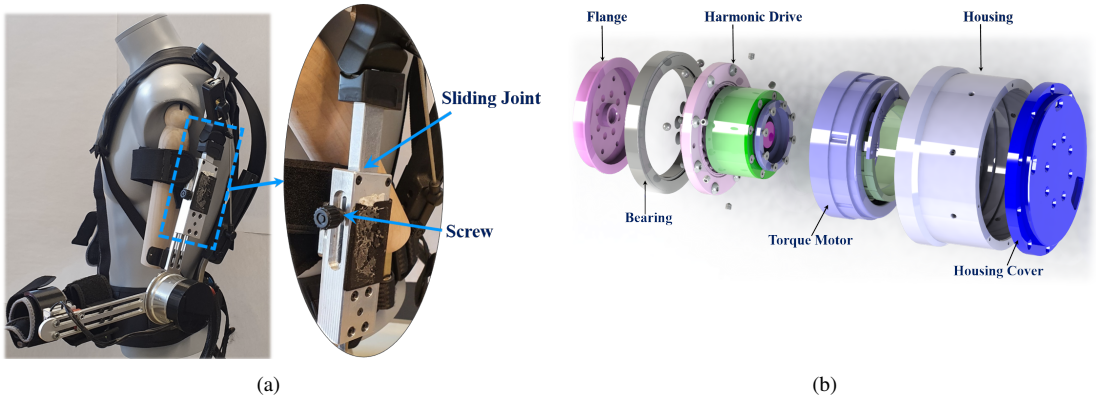

(a) (b)

Figure 2. Demonstration of the hybrid exoskeleton design integration. (a) Integration of Skelex 360 with low power active elbow joint module using a sliding joint. (b) Exploded view of the custom made driving unit for elbow joint.

type of exoskeletons that combine both active assistive mode and passive assistive mode with gravity compensation. The purpose of the hybrid exoskeleton is to facilitate the user in performing several industrial tasks, including overhead load-lifting while maintaining a prolonged body posture, transporting a load to a shorter distance, or enable the user to interact with the heavy objects by providing a modulated assistive torque profile. Thus, it can be hypothesized that the concept of using a low power hybrid exoskeleton will complement the users in different task conditions throughout the work shift and reduces the physical human effort.

In this paper, a dynamic model of a hybrid upper limb exoskeleton is developed. Upon the model developed, simulations of load-lifting tasks are perform to study the effect of exoskeleton on human upper limb model. The main focus of this work is expressed as follows:

1) Investigating the efficacy of hybrid exoskeleton to reduce the human effort.

2) Analyzing the load sharing between the human and exoskeleton for the different levels of assistance.

The effectiveness of using a hybrid exoskeleton in an industrial environment, such as lifting and transporting the object, is investigated using the multibody modeling approach. The study also presents an analysis of personalized forearm assistance by dynamically varying the assistive torque profile.

The rest of this paper is organized as follows. Modeling of the hybrid exoskeleton is introduced in Section II. Its kinematics and dynamics are also modeled to see its response in operational space. Further, the energy sharing is investigated for the different levels of assistive torques in Section III. Subsequently, comparisons among different parameters and scenarios are also illustrated in Section IV. Finally, conclusions and future directions are given in Section V.

A Hybrid Exoskeleton

Mechanical Design

The exoskeleton in Fig. 1 is built with a passive shoulder joint and an active elbow joint. The passive shoulder joint is designed on the biases of a commercially available exoskeleton called Skelex 360, which is developed to counterbalance the gravity torque and support the user in performing the overhead industrial tasks and all kinds of upper arm elevation tasks. For this purpose, two flat extension springs are inserted on the backside to store the kinetic energy when lowering the upper arm. This spring-loaded shoulder mechanism can be adjusted to achieve the desired torque profile to obtain minimal energy consumption by maximizing the gravity compensation.

In the hybrid exoskeleton arm, the elbow joint is designed with a custom-made integrated driving unit, that can provide a maximum torque of 50 Nm. The driving unit was initially designed to support physically impaired people in another possible application, such as sit-to-stand motion amplification, for which 50 Nm is torque is needed. The integrated driving unit consists of a customized permanent magnet torque motor and a harmonic drive (speed reducer) with a high gear ratio of 1:100. An exploded view of the custom-made driving unit is shown in Fig. 2b. A 12-bit absolute magnetic encoder (AS5145B) is also used to record the rotational angle. The whole driving unit is developed by carefully considering the weight and the dimensional

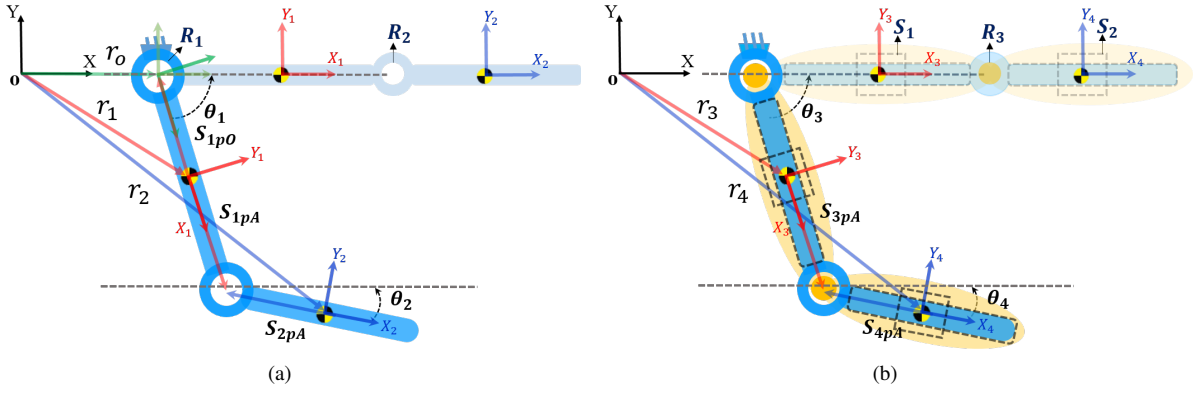

Figure 3. Geometrical model of a multibody assistive exoskeleton. The blue structure represents the exoskeleton, whereas the yellow body represents a simplified model for the human upper limb skeletal system. (a) Illustration of the geometrical model for the robotic exoskeleton system with the local and global position vectors. R_1 is the revolute joint defined between ground and exoskeleton upper arm, while R_2 is the revolute joint between the exoskeleton upper arm and forearm. (b) Illustration of the geometrical model with the inclusion of the human upper limb. S_1 and S_2 are the two sliding joints that connect the human upper limb model and exoskeleton to from a closed-loop system. The human elbow is defined by the revolute joint R_3.

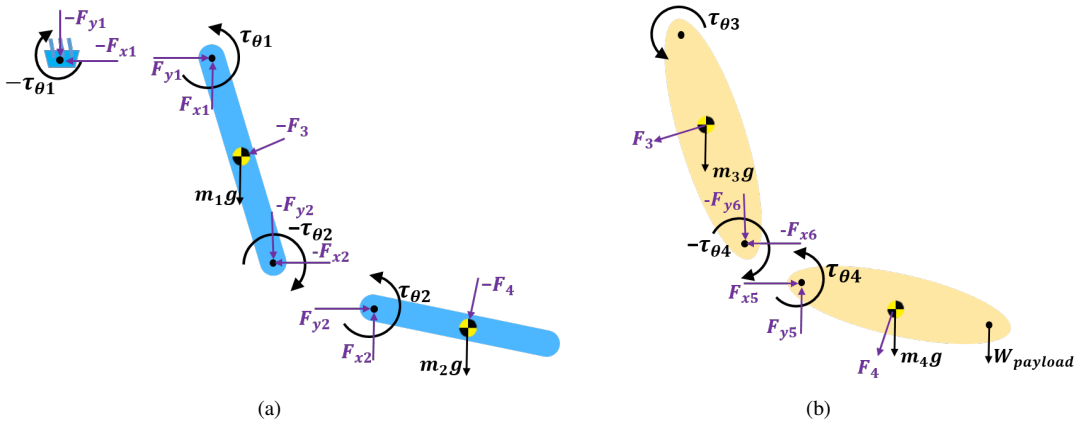

Figure 4. Force diagram for robotic exoskeleton and the simplified human upper limb skeletal system. (a) $\tau_{\theta 1}$ and $\tau_{\theta 2}$ are the assistive torques generated by the exoskeleton shoulder and elbow joints, respectively. (b) $\tau_{\theta 3}$ and $\tau_{\theta 4}$ are the driving torques generated by the human upper limb model. F_3 and F_4 are the forces generated by the interaction between the multibody human-exoskeleton system with the two sliding joints. F_3 and F_4 will always be perpendicular to the exoskeleton upper and forearm, respectively.

requirements. Hence, the final design has a dimension of $D72mm \times 48mm$ and weighs $600g$.

The whole system weighs around 5 Kg, excluding batteries. An overall integration of the Skelex 360 with the active elbow joint module is presented in Fig. 2a. This method of combining the Skelex 360 with an actively actuated elbow joint module can support the user not only in the overhead lifting tasks but also facilitate them in transferring the different types of the loads from one location to another by providing a modulated assistive torque at the elbow joint and helps to minimize physical human effort.

- **Assumption I:** The human upper limb model is approximated as a rigid body and the deformation of the soft parts are not considered.
- **Assumption II:** The motion is confined in the sagittal plane.

The constraints between the human upper limb and the exoskeleton are established as

$$\Phi(\mathbf{q}) = \begin{Bmatrix} \mathbf{r}_0 - \mathbf{r}_1 - \mathbf{A}_1\mathbf{s}_{1pO} \\ \mathbf{r}_1 + \mathbf{A}_1\mathbf{s}_{1pA} - \mathbf{r}_2 - \mathbf{A}_2\mathbf{s}_{2pA} \\ \mathbf{r}_3 + \mathbf{A}_3\mathbf{s}_{3pA} - \mathbf{r}_4 - \mathbf{A}_4\mathbf{s}_{4pA} \\ (\mathbf{A}_1\mathbf{u})^T(\mathbf{r}_3 - \mathbf{r}_1) \\ \theta_3 - \theta_1 \\ (\mathbf{A}_2\mathbf{u})^T(\mathbf{r}_4 - \mathbf{r}_2) \\ \theta_4 - \theta_2 \end{Bmatrix} = 0 \qquad (1)$$

where $\mathbf{r}_i$ is the global vector defining the joint locations, and $\mathbf{A}_i$ and $\mathbf{s}_i$ represent the rotation matrix and local vector. The geometrical model for the multibody system can be found in Fig. 3 (a & b).

Finally, the dynamic response of this multibody closed-loop system is modeled with Lagrange multiplier approach (*20*). Besides investigating the torque profiles, this modeling method is advantageous in analyzing the interaction between human and exoskeleton in terms of contact forces.

$$\mathbf{M}\ddot{\mathbf{q}} - \mathbf{D}^T\boldsymbol{\lambda} = \mathbf{g} \qquad (2)$$

where $\mathbf{M}$ and $\ddot{\mathbf{q}}$ is the mass matrix and the acceleration, respectively. $\mathbf{D}$ is the system's jacobian matrix derived from the constraint equation Eq. 1. $\boldsymbol{\lambda}$ is an array the Lagrange multipliers. $\mathbf{g}$ is an array of gravitational and external forces and the external torques. Fig. 4 shows all the of torques and forces acting on the individual body. The kinematic and the mass inertia properties selected for this study are given in Appendix I.

Spring Force Modeling

The exoskeleton passive shoulder joint is modeled as a hinged lever constant force mechanism. This mechanism can support the user to compensate for the gravitational force or the human arm weight.

$$F_s L_{S1} sin\theta - F_o L_{S2} sin\alpha = 0 \qquad (3)$$

According to the Hooke's law.

$$F_s = k \cdot \delta. \qquad (4)$$

where k and δ are the spring constant and displacement of linear spring respectively. For a structure shown in the Fig. 5, δ can be found by using sine law.

$$\delta = L_{S4} = L_{S3}\frac{sin\alpha}{sin\theta} \qquad (5)$$

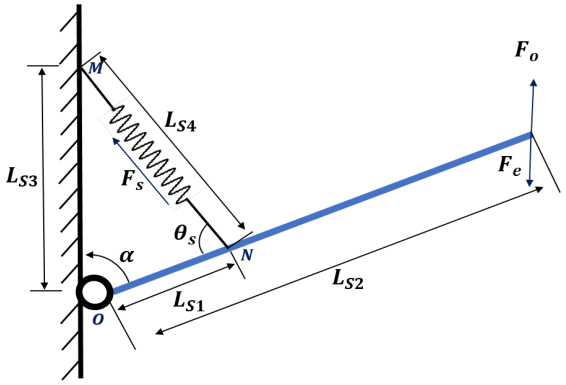

Figure 5. Schematic diagram of the hinged-lever constant force mechanism.

The torque contribution of this spring can be expressed as.

$$\tau_s = F_s L_{S1} sin\theta \tag{6}$$

This hinged lever constant force spring is used to model the exoskeleton shoulder joint torque where it can passively support the wearier in performing upper arm elevation tasks as shown in Fig. 6. This assistive torque is then used to compute the other unknown joint torques and forces.

Multibody Modeling

The hybrid exoskeleton interacts with the human upper limb for the purpose of motion amplification and combines to from a multibody system. In modeling the kinematics of human exoskeleton system, the following assumptions are made:

Interaction Forces Model and Load Sharing between Human and Exoskeleton

The attachment between human and exoskeleton is modeled as a sliding/translational joint represented by S_1 and S_2, as shown in Fig. 3b. The interaction forces are found as

$$\mathbf{g}^{(c)} = \mathbf{D_q}^T \boldsymbol{\lambda} \tag{7}$$

where $\mathbf{D_q}^T$ is the transpose of the constraint jacobian matrix. The torque values obtained by solving Eq (2) will give the maximum values for a multibody system. It means that the human shoulder joint and exoskeleton elbow joint move with maximum torques. However, in a real case scenario, an exoskeleton robot should be able to provide a variable amount of torque to assist the movement as required by the human, so called assistive torques. Hence, Eq (2) will be solved for $\tau_{\theta 3}$ and $\tau_{\theta 2}$ for the known values of $\tau_{\theta 1}$ and $\tau_{\theta 4}$ as shown below.

$$\begin{aligned} \tau_{\theta 1} &= F_s L_{S1} sin\theta_s \\ \tau_{\theta 4} &= \tau_{payload} \cdot K \qquad\qquad 0 \leq K \leq 1 \end{aligned} \tag{8}$$

where $\tau_{\theta 1}$ is the assistive torque generated by the exoskeleton shoulder joint. F_s is the spring force obtained from (4) and k is the value for the spring constant. $\tau_{\theta 4}$ is the driving torque produced by the human forearm in handling. K dictates the different level of assistance provided by the exoskeleton elbow joint and it varies from 0 to 1 depending upon the level of assistance. This level of assistance will be measured as a percentage of the maximum torque that $\tau_{\theta 2}$ can provide. It is noted that the exoskeleton shoulder joint is equipped with the constant force spring mechanism and can not provide the different assistance level.

Case Studies

In this section, the performance of multibody human exoskeleton system in the motion assistance is simulated. Two tasks are considered: An overhead lifting task and a load transferring task using a payload of $3kg$, both shown in Fig. 6 and Fig. 11. The spring constant selected for the passively actuated shoulder mechanism is $k = 45N/m$.

CASE I (Overhead lifting task)

In the 1st case, a payload of $3kg$, shown in Fig. 6a, is applied to the multibody system. The human exoskeleton system performs an overhead lifting task in the sagittal plane, as shown in Fig. 6b, with the joint trajectories displayed in Fig. 7.

The motion trajectory is defined as

$$\begin{aligned} \theta_1(t) = \theta_3(t) &= -\tfrac{\pi t^3}{27} + \tfrac{\pi t^2}{6} - \tfrac{\pi}{2} \\ \theta_2(t) = \theta_4(t) &= -\tfrac{\pi t^3}{54} + \tfrac{\pi t^2}{12} \end{aligned} \tag{9}$$

Upon the given trajectories, several forces and the torques are acting on the multibody human exoskeleton system, however, we have only chose to present Figs. 8 and 9 that display the interaction forces (F_3 and F_4), the assistive torques ($\tau_{\theta 1}$ and $\tau_{\theta 2}$), and the driving torques ($\tau_{\theta 3}$ and $\tau_{\theta 4}$).

At $t = 0s$, an upper limb human exoskeleton system maintains its initial position, i.e., the human upper arm and forearm maintains an orientation of $-90°$ and $0°$,

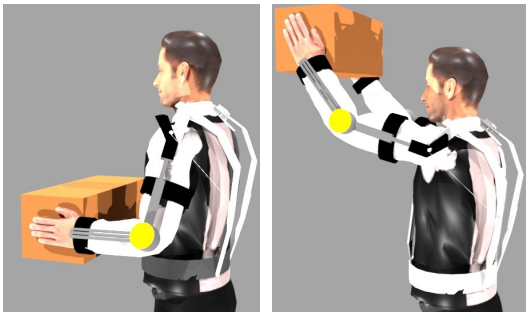

(a) 0 s (b) 3 s

Figure 6. Demonstrations of overhead lifting task with $3kg$ payload.

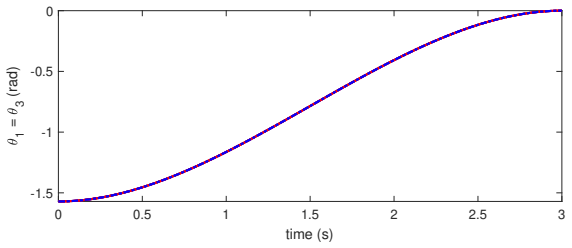

(a) Shoulder joint trajectories

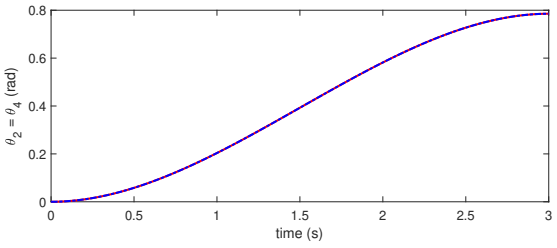

(b) Elbow joint trajectories

Figure 7. Exoskeleton and human joint angle trajectories for overhead lifting task. (a) θ_1 and θ_3 represent the exoskeleton and human shoulder joint trajectories, respectively and (b) θ_2 be the exoskeleton's elbow joint angle and θ_4 represents the human elbow joint angle.

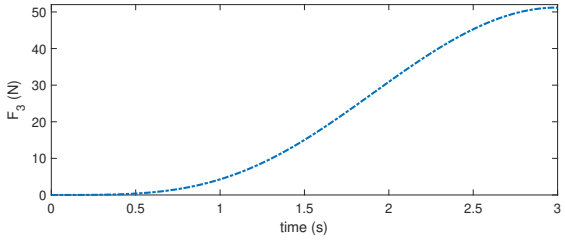

(a) Interaction force between exoskeleton and human upper arm

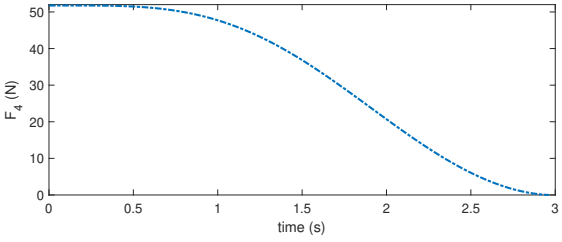

(b) Interaction force between exoskeleton and human forearm

Figure 8. Interaction forces between the human and exoskeleton while performing a over head task. (a) F_3 is the interaction force between exoskeleton and human upper arm, and (b) F_4 is interaction force between exoskeleton and human forearm.

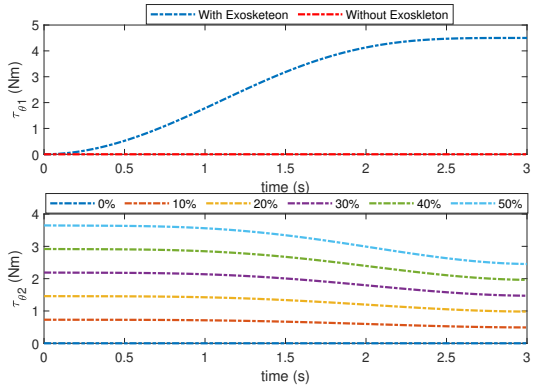

(a) Exoskeleton applied torques profiles

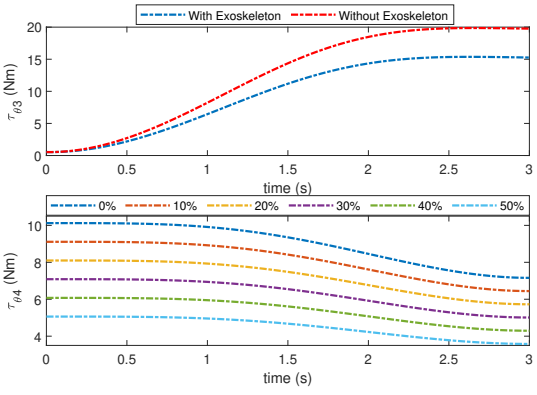

(b) Human upper limb torques profiles

Figure 9. Torque profile for a closed loop multibody system while performing an overhead task. (a) $\tau_{\theta 1}$ and $\tau_{\theta 2}$ are the applied torques by the exoskeleton shoulder and elbow joint respectively, and (b) $\tau_{\theta 3}$ and $\tau_{\theta 4}$ are the actual torques generated by the human.

respectively, shown in Fig. 6a. At this orientation, the interaction force F_3 between the human upper arm model and exoskeleton is zero, while the human forearm model experiences a maximum interaction force $(F_4 = 51.76N)$. When the human arm starts moving toward the final position, it is observed that the interaction force between the human upper arm model and exoskeleton system starts increasing, i.e., the magnitude of F_4 decreases. Once the human hand/end-effector attains the final position, the magnitude of the force $(F_3 = 51.17N)$ is maximizes, shown in Fig.

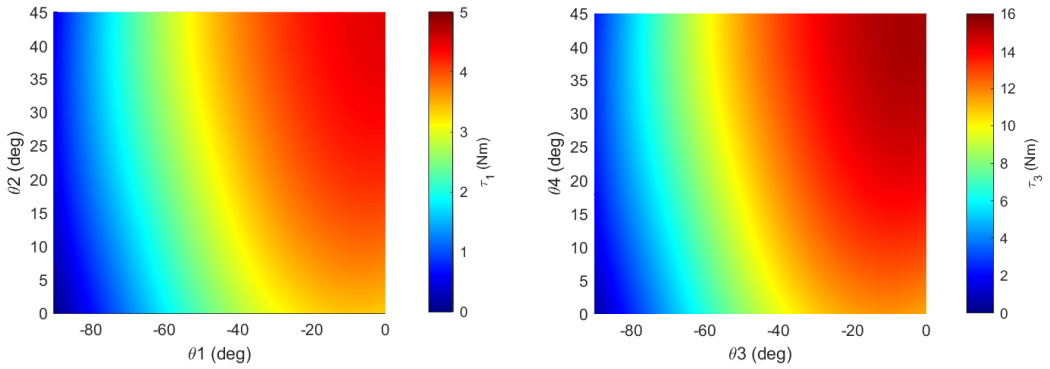

(a) Exoskeleton shoulder joint torque (b) Human shoulder joint torque

Figure 10. Exoskeleton and human arm workspace and shoulder joint torques analysis using contour plots for overhead lifting task. (a) Exoskeleton shoulder joint torque for human arm weight compensation, and (b) Required human shoulder joint torque in the presence of exoskeleton assistance.

8a. At this orientation, all forces (gravity, payload, and weight) have maximized their effect on the upper arm human model and caused to induce the physical strain in case of insufficient amount of the assistive torque provided by the exoskeleton system. However, the magnitude of F_4 is minimum, so the human forearm remains less prone to the fatigue. The interaction between the human upper limb model and exoskeleton system can be seen in Fig. 8.

It is noted that the interaction between human and exoskeleton depends not only on the contact forces but also on the assistive/driving torques. In the real-time scenario, the exoskeleton must be able to provide a variable amount of torque to supplement the user. Thus, it is required to analyze the mathematical model for the different levels of assistive torques. These different levels of assistive torque are defined as the percentage of total torque the exoskeleton can provide, as shown in (8). However, the exoskeleton shoulder joint can passively support the wearer to compensate for the human arm weight. The level of assistance provided by the exoskeleton to the human shoulder joint remained the same. This exoskeleton shoulder joint complements the human upper arm model in the overhead lifting task and reduces the physical human effort by 20%. As a result, the peak torque of human shoulder $(\tau_{\theta 3})$ is also reduced from $19.77Nm$ to $15.37Nm$, as can be seen from Fig. 9 (a & b). This reduction in the physical human effort is measured from $\tau_{\theta 3}$ for the given two conditions on $\tau_{\theta 1}$:

1. **Condition I:** $\tau_{\theta 1} = F_s L_{S1} sin\theta_s$
   Execution of an overhead lifting task with exoskeleton support.
2. **Condition II:** $\tau_{\theta 1} = 0$
   Execution of the overhead lifting task without exoskeleton support.

Upon the given two conditions, we have analyzed the dynamic response of the human upper limb model with and

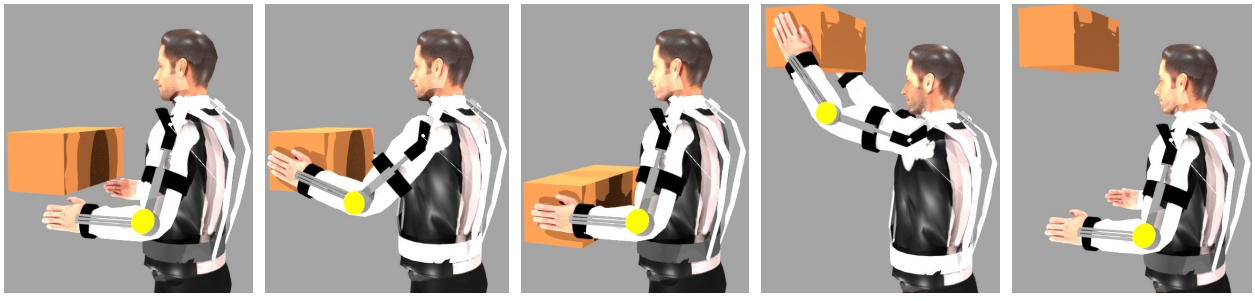

(a) t = 0 s (b) t = 3 s (c) t = 6 s (d) t = 9 s (e) t = 12 s

Figure 11. Demonstrations of load lifting task: from time 0 to 3s, the exoskeleton assists the human arm in approaching toward the payload; from 4s to 6s, the human picks the payload and get back to the initial position.; from 7s to 9s, the human arm transfers the payload to a shelf located at a specific height; from 10s to 12s, the human arm gets back to the initial position.

without the exoskeleton's passive assistance, as shown in Fig. 9. Fig. 10(a) show the contour plot for exoskeleton shoulder joint with the variation in θ_1 and θ_2, while Fig. 10(b) shows the contour plot for human shoulder joint with the variation in θ_3 and θ_4. These contour plots helped us to identify the critical points on the trajectory where $\tau_{\theta 1}$ and $\tau_{\theta 3}$ values would be maximum. For instance, in Fig. 10(b) $\tau_{\theta 2}$ is maximum at $\theta_3 = 0^\circ$ and $\theta_4 = 45^\circ$ that corresponds to the flexion of human upper arm and forearm model. Moreover, the combined effect of upper arm and forearm movements on the human-exoskeleton shoulder joint can be clearly seen from these plots.

The exoskeleton's elbow joint can actively support the human forearm movements and provides variable assistance levels. In order to analyze the assistive torques as well as the load sharing between human and exoskeleton system, six different assistance levels are considered as shown in Fig. 9. The assistive torque at the elbow joint is varied from 0% to 50% while performing the overhead lifting task in the sagittal plane. As a result, the peak human elbow joint torque is reduced from $10.12Nm$ to $5.1Nm$.

CASE II

In the second case, a complete picking and placing or a dynamic load transferring task is simulated with the closed loop human exoskeleton system in the sagittal plane, as shown in Fig. 11. To simplify the notation, we call it a "Load transferring task." In this task, an exoskeleton is complementing the human arm model in approaching toward the payload as shown in Fig. 11 (a & b); this is simulated from 0 second (s) to 3 seconds. From 4s to 6s, the human upper limb model picks the payload and get back to the initial position. Thereafter, from 7s to 9s, the human-exoskeleton system transfers the payload to a shelf located at a specific height, and from 10s to 12s, the human-exoskeleton model gets back to its initial position. Fig. 12 shows the joint angle trajectories with the equations given in Appendix II.

In the beginning, the exoskeleton tried to support the human upper limb model for maintaining its initial position, at $t = 0s$ the orientations of the human upper arm and forearm models were be -90° and 0°, respectively, shown in Fig. 11a. The interaction force F_3 between the upper arm model and exoskeleton system is zero, while interaction force on the human forearm is noticed to be higher $(F_4 = 22.30N)$. At $t = 3s$, the human upper limb model starts picking up the pay load of $3kg$, as it can be seen in Fig. 11b, which causes a sudden increase in the contact force F_4 between human-exoskeleton system and the forearm driving torques $\tau_{\theta 2}$ and $\tau_{\theta 4}$, shown in Fig. 14. At this orientation, the magnitude of F_4 is significantly high $(F_4 = 48.53N)$

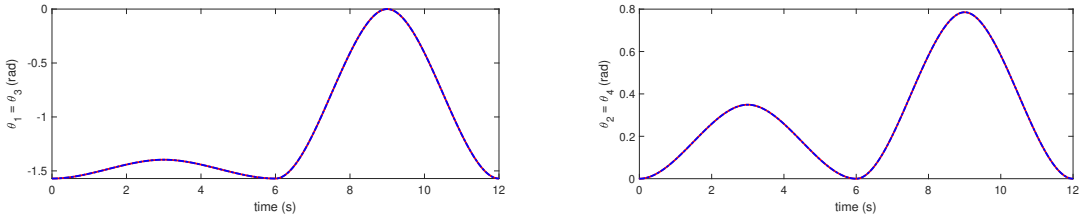

(a) Shoulder joint trajectories (b) Elbow joint trajectories

Figure 12. Exoskeleton and human joint angle trajectories for load transferring task in 12 seconds. (a) θ_1 and θ_3 represent the exoskeleton and human shoulder joint trajectories, respectively and (b) θ_2 be the exoskeleton's elbow joint angle and θ_4 represents the human elbow joint angle.

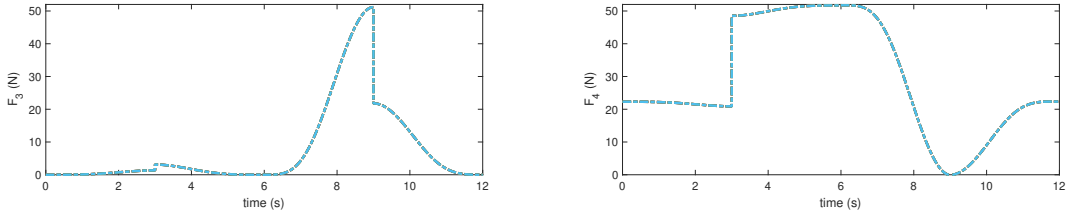

(a) Interaction force between exoskeleton and human upper arm (b) Interaction force between exoskeleton and human forearm

Figure 13. Interaction forces between the human and exoskeleton while performing a load transferring task in 12 seconds. (a) F_3 is the interaction force between exoskeleton and human upper arm, and (b) F_4 is the interaction force between exoskeleton and human forearm.

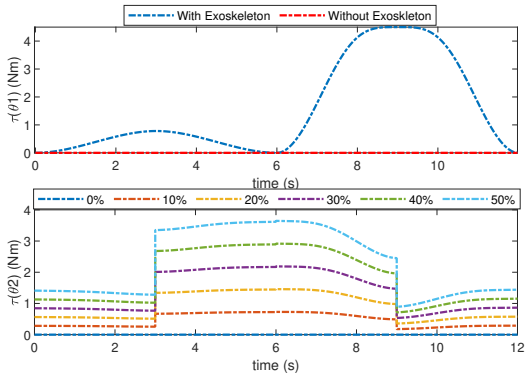

(a) Driving torque of exoskeleton for different levels of assistance.

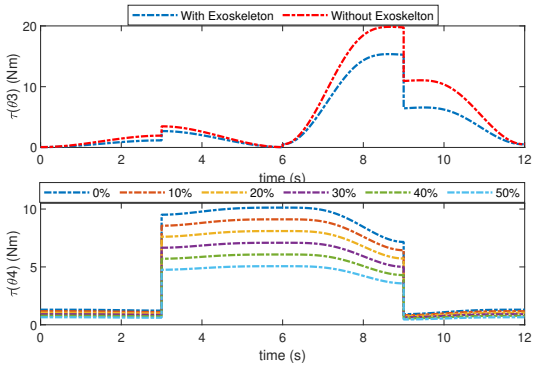

(b) Driving torque of human for different levels of assistance.

Figure 14. Driving torques for human and exoskeleton while performing a load transferring task. The torques required for exoskeleton and human for different levels of assistance are presented in term of percentage. (a) $\tau_{\theta 1}$ and $\tau_{\theta 2}$ are the driving torques of exoskeleton's shoulder and elbow joints, respectively. and (b) $\tau_{\theta 3}$ is the driving torque for human shoulder joint and $\tau_{\theta 4}$ is the driving torques for human elbow joint.

as the effect of payload is found to be more prominent on the contact point between human and exoskeleton forearm model, as shown in the Fig. 13. When this human exoskeleton system tries to transfer the load at a certain height as shown in Fig. 11d, the interaction force between human and exoskeleton upper arm model is found to be maximum $(F_3 = 51.17N)$. Once the payload transfers to the allocated height, the system attains its initial position, as shown in Fig. 11c. A large variation in F3 can be noticed at $t = 9s$, shown in Fig. 13b. The sharp drop in driving torque of human forearm and exoskeleton is seen at $t = 9s$, which corresponds to the load releasing. The change of condition is also seen in Fig. 14.

For the given scenario, the exoskeleton shoulder joint can passively support the human upper limb model to compensate for human arm weight. It is noticed that when the exoskeleton started complementing the human shoulder joint, the peak physical human effort has reduced by 20%. As a result, the maximum human shoulder joint torque $(\tau_{\theta 3})$ is dropped from $19.77Nm$ to $15.37Nm$ while performing a load transferring task shown in Fig. 14. The method of measuring and comparing the exoskeleton assistance to the human upper arm model has already been explained in the previous section. Moreover the exoskeleton can actively support the human forearm extension/flexion. Therefore, six different assistance levels are considered to analyze the load sharing and the effectiveness of variable assistive torque $(\tau_{\theta 2})$ on the human upper limb model. These assistance levels are defined as the percentage of total torque the exoskeleton can provide, as shown in Fig. 14. When this assistive torque is varied from 0% to 50%, it is noted that the peak human effort is reduced from $10.12Nm$ to $5.1Nm$.

Discussion

In this paper, a dynamic model of a hybrid upper limb exoskeleton is presented using a multibody modeling approach. A force model based on the Lagrange multiplier approach and joint torques were used to study the complicated interaction in which an exoskeleton's movement is coupled with the human arm motion. Two different tasks were simulated to analyze the reduction in the physical human effort subject to the different levels of assistance provided by the hybrid exoskeleton were also investigated, as presented in the previous case studies. In this work, the reduction in the physical human effort is associated with the higher assistance level(*15*). Several user activities were analyzed in an industrial environment for the selection of critical tasks. It shows that the overhead lifting tasks by maintaining a prolonged posture and load transferring tasks for a longer interval could induce some signs of musculoskeletal fatigue or MSD. For an overhead lifting task, initially, the interaction forces between the human and exoskeleton forearms were maximum compared to the upper arm, as shown in Fig. 8. At this orientation, the human forearm will more likely experience musculoskeletal fatigue in case of high payload or maintaining this posture for a longer interval of time. Similarly, when the human upper limb model carrying a payload of $3kg$ tried to approach at its final position as shown in Fig. 6, the interaction force between the human upper arm and exoskeleton was noticed to be maximum. In the case of excessive loading, the human may experience an uncomfortable interaction at the upper arm. This human-exoskeleton interaction can be improved by optimizing the design parameters. Apart from the interaction forces, assistive torques provided by the hybrid exoskeleton also caused to suppress the musculoskeletal fatigue at the

human shoulder and elbow joints. The results have shown the significance of using a hybrid exoskeleton where the human upper arm maximum effort was reduced by 20%. Moreover, the active assistance provided by the exoskeleton to the human forearm has reduced the human driving torque from $10.12Nm$ to $5.1Nm$

The hybrid exoskeleton took the advantage of both passive and active mechanism and maximized its energy balance by improving the human robot interaction (*21*). The shoulder joint of hybrid exoskeleton is a passive compliant joint which not only supports the user but also enhances the shock tolerance capacity and prevents the user from inelastic collision force spikes. Moreover, to improve the power efficiency of the multibody system, it is required to optimize the assistive torques (*22*). Usually the exoskeletons are designed to operate at low speed and the dominant torque is to carry the human arm and payload. It is therefore beneficial to counterbalance the effect of gravitational torque or human arm weight to save a significant amount of mechanical energy using some elastic element. The spring loaded passive shoulder mechanism of the hybrid exoskeleton works on the same principle and support the user in counter balancing the gravitational torque. However, the elbow joint of hybrid exoskeleton can actively support the user forearm extension/flexion. The compactness of the elbow joint and its precise manipulation is achieved by considering a direct drive method in the design phase.

Reduction in peak power, effective energy consumption provided the stiffness of spring element is appropriately tuned, and the precise motion control of elbow joint are the main advantages of combining passive and active mechanisms (*21*). The concept of using a hybrid exoskeleton in industrial settings would not only facilitate the user in an overhead lifting task but helps them in other industrial applications that need to support the human elbow joint by providing a modulating torque profile. From the data presented in the above two case studies, it is perceived that the hybrid exoskeleton can be used to improve the physical human performance in different task conditions throughout the work shift and mitigate the large variation in fatigue level.

Compared with existing works on exoskeleton design and modeling, the work presented in this paper show originality in the following perspectives:

1. A hybrid exoskeleton combining an active elbow joint and a passive shoulder joint with gravity compensation is introduced.
2. A dynamic model is developed in connection with the hybrid exoskeleton, in which assistance level is considered to account for the influence of spring stiffness and the power level on the exoskeleton performance.
3. The dynamic model can be used for a variety of purposes, including (1) parametric study for the exoskeleton design optimization, (2) selection of the actuator, specifically, it helps in the optimal selection of elastic element for the passively actuated exoskeleton mechanism, (3) simulation of the different working conditions to access the dynamic performance.

In the future, more simulation and analysis, preferably with the experimental validation are required to identify the response of human upper limb model with the robotic assistance. For a better understanding of the physical human robotic interaction, following points would be considered for the performance evaluation.

1. Evaluate the reduction in physical human effort by recording an EMG data from human upper limb with and without exoskeleton.
2. Duration of the task along with the workspace would be evaluated because several lengthy tasks may reduce the user workspace and human may experience some signs of musculoskeletal fatigue. For example, Kim et al. (*16*) reported that the Ekso Vest has reduced the movement completion time by 19% during an overhead drilling task.
3. Investigate that how deliberately the human can change it movement strategy using passive mechanism. A study on Airframe has shown that the participants are facing difficulty in maintaining an abducted arm posture (*23*).

Conclusions

This study presents a dynamic model of an upper limb hybrid exoskeleton using multibody modeling approach. The model is used to analyze the human-exoskeletal interaction by looking at the contact forces for overhead and load transfer tasks. These contact forces are used to identify the critical point on the trajectory, where the human upper limb model may experience maximum interaction forces i.e $F_3 = 51.17N$ and $F_4 = 51.76N$. If the human upper limb tried to maintain a prolonged posture or exposed to the higher external forces, the critical points on the trajectory may cause musculoskeletal strain or fatigue, which should be avoided in practical works. Moreover, the load sharing between the human upper limb model and exoskeleton was also analyzed for the different level of assistance. The modeling results show that the hybrid exoskeleton has reduced the maximum human shoulder joint torque by 22.65%. In addition, the personalized forearm assistance by varying torque profile (from 0% to 50%) has reduced the peak human forearm effort from 10.12 Nm to 5.1 Nm. These results imply that the use of hybrid exoskeleton will help to reduce the human physical effort in an industrial environment and prevent the work related MSDs. Experimental verification of this assistive effect will be a topic of future study of continuation of current research works.

Declaration of Conflicting Interests

The author(s) declared no potential conflicts of interest with respect to the research, authorship, and/or publication of this article.

Acknowledgment

This work is supported in part by Innovative Fund Denmark Grand Solutions project Exo-aider and AAU EXOTIC project. The authors acknowledge the support of Harun Leto for his participatiion and helping us in developing the mathematical model.

Appendix I

Table 1. Mechanical properties of upper limb hybrid exoskeleton model and anthropomorphic parameters of a human Upper limb model.

Link	I_{zz} (kg.m^2)	mass (kg)	Length (m)	Center of Mass
Hybrid Exoskeleton				
Upper arm	0.20	2.5	0.3	0.10
Forearm	0.15	1.5	0.3	0.10
Human Upper Limb Model				
Upper arm	0.0416	1.386	0.3	0.15
Forearm	0.0266	0.886	0.3	0.15

Appendix II

Following joint trajectories are obtained For load transferring task shown in Fig. 11:
$t \in 1 \rightarrow 3sec$

$$\theta_1(t) = \theta_3(t) = -\frac{\pi t^3}{243} + \frac{\pi t^2}{54} - \frac{\pi}{2}$$
$$\theta_2(t) = \theta_4(t) = -\frac{2\pi t^3}{243} + \frac{\pi t^2}{27}$$

$t \in 4 \rightarrow 6sec$

$$\theta_1(t) = \theta_3(t) = \frac{\pi t^3}{243} - \frac{\pi t^2}{54} - \frac{4\pi}{9}$$
$$\theta_2(t) = \theta_4(t) = \frac{2\pi t^3}{243} - \frac{\pi t^2}{27} + \frac{\pi t^2}{9}$$

$t \in 7 \rightarrow 9sec$

$$\theta_1(t) = \theta_3(t) = -\frac{\pi t^3}{27} + \frac{\pi t^2}{6} - \frac{\pi}{2}$$
$$\theta_2(t) = \theta_4(t) = -\frac{\pi t^3}{54} + \frac{\pi t^2}{12}$$

$t \in 10 \rightarrow 12sec$

$$\theta_1(t) = \theta_3(t) = \frac{\pi t^3}{27} - \frac{\pi t^2}{6}$$
$$\theta_2(t) = \theta_4(t) = \frac{2\pi t^3}{54} - \frac{\pi t^2}{12} + \frac{\pi}{4}$$

The trajectories are graphically displayed in Fig. 12.

References

1. de Looij Ivo. Modeling and altering the force profile of a spring-based upper body exoskeleton with design adjustments. *TU Delft, Netherlands*, (2017).
2. de Vries A, de Looze M. The effect of arm support exoskeletons in realistic work activities: A review study. *J Ergonomics* 2019; 9:255.
3. de Kok J, Vroonhof P, Snijders J, et al. Work-related musculoskeletal disorders: prevalence, costs and demographics in the EU. *Eupropean Risk Observatory Report. Luxembourg: European Agency for Safety and Health at Work (EU-OSHA)* 2019.
4. Teng L, Gull MA, Bai S. PD-Based Fuzzy Sliding Mode Control of a Wheelchair Exoskeleton Robot. *IEEE/ASME Transactions on Mechatronics* 2020; 25.5: 2546-2555.
5. Kim B, Deshpande AD. An upper-body rehabilitation exoskeleton Harmony with an anatomical shoulder mechanism: Design, modeling, control, and performance evaluation. *The International Journal of Robotics Research* 2017; 36.4: 414-435.
6. Lee S, Lee S, Na Y, et al. Shock absorber mechanism based on an SMA spring for lightweight exoskeleton applications. *International Journal of Precision Engineering and Manufacturing* 2019; 20.9: 1533-1541.
7. Hong MB, Kim GT, Yoon YH, et al. Ace-ankle: A novel sensorized rcm (remote-center-of-motion) ankle mechanism for military purpose exoskeleton. *Robotica* 2019; 37.12: 2209-2228.
8. Gull MA, Bai S, Bak T. A review on design of upper limb exoskeletons. *Robotics* 2020; 9.1: 16.
9. S Christensen and S Bai. Kinematic Analysis and Design of a Novel Shoulder Exoskeleton using a Double Parallelogram Linkage, *ASME J. Mechanisms and Robotics* 2018; 10.4: 041008.
10. Castro MN, Rasmussen J, Andersen MS, et al. A compact 3-DOF shoulder mechanism constructed with scissors linkages for exoskeleton applications. *Mechanism and Machine Theory* 2019; 132: 264-278.
11. Hyun DJ, Bae K, Kim K, et al. A light-weight passive upper arm assistive exoskeleton based on multi-linkage spring-energy dissipation mechanism for overhead tasks. *Robotics and Autonomous Systems* 2019; 122: 103309.
12. Nasiri R, Ahmadi A, Ahmadabadi M N. Reducing the energy cost of human running using an unpowered exoskeleton. *IEEE Transactions on Neural Systems and Rehabilitation Engineering* 2018; 26.10: 2026-2032.
13. Kim HG, Lee JW, Jang J, et al. Design of an exoskeleton with minimized energy consumption based on using elastic and dissipative elements. *International Journal of Control, Automation and Systems* 2015; 13.2: 463-474.
14. De Looze MP, Bosch T, Krause F, et al. Exoskeletons for industrial application and their potential effects on physical work load. *Ergonomics* 2016; 59.5: 671-681.

15. Grazi L, Trigili E, Proface G, et al. Design and experimental evaluation of a semi-passive upper-limb exoskeleton for workers with motorized tuning of assistance. *IEEE Transactions on Neural Systems and Rehabilitation Engineering* 2020; 28.10: 2276-2285.
16. Kim S, Nussbaum MA, Esfahani MIM, et al. Assessing the influence of a passive, upper extremity exoskeletal vest for tasks requiring arm elevation: Part I - "Expecte" effects on discomfort, shoulder muscle activity, and work task performance. *Applied ergonomics* 2018; 70: 315-322.
17. Alabdulkarim S, Nussbaum MA. Influences of different exoskeleton designs and tool mass on physical demands and performance in a simulated overhead drilling task. *Applied ergonomics* 2019; 74: 55-66.
18. Pacifico I, Scano A, Guanziroli E, et al. An experimental evaluation of the proto-mate: a novel ergonomic upper-limb exoskeleton to reduce workers' physical strain. *IEEE Robotics Automation Magazine* 2020; 27.1: 54-65.
19. Bai S, Rasmussen J. Modelling of physical human-robot interaction for exoskeleton designs. *In Proc. of Multibody Dynamics 2011, ECCOMAS Thematic Conference*, Brussels, Belgium, 4-7 July 2011.
20. Nikravesh PE. Computer-aided analysis of mechanical systems. Prentice-Hall Inc. 1988.
21. Kashiri N, Abate A, Abram SJ, et al. An overview on principles for energy efficient robot locomotion. *Frontiers in Robotics and AI* 2018; 5: 129.
22. Beckerle P, Verstraten T, Mathijssen G, et al. Series and parallel elastic actuation: Influence of operating positions on design and control. *IEEE/ASME Transactions on Mechatronics* 2016; 22.1: 521-529.
23. Spada S, Ghibaudo L, Gilotta S, et al. Analysis of exoskeleton introduction in industrial reality: main issues and EAWS risk assessment. *In International Conference on Applied Human Factors and Ergonomics.* Springer, Cham 2017; 236-244.